ELSEVIER

Catalysis Today 53 (1999) 289–302

CATALYSIS TODAY

www.elsevier.com/locate/cattod

Monte Carlo simulations of heterogeneous catalytic reactions on highly dispersed supported metal catalysts

A.S. McLeod *

School of Chemical Engineering, University of Edinburgh, King's Buildings, Mayfield Road, Edinburgh, EH9 3JL, Scotland

Abstract

The influence of catalyst geometry and topology on two model catalytic reactions, the hydrogenation of alkenes and the oxidation of carbon monoxide, has been studied by Monte Carlo simulation. We discuss the application of an efficient algorithm for simulating catalytic reactions in cases where diffusion of adsorbate molecules occurs on both the catalyst support and the metal particles. We first consider the influence of metal particle size and geometry on the kinetics of a series of hydrocarbon hydrogenation reactions and demonstrate that the reaction kinetics can be described by an extension of the ensemble theory. This result is in agreement with previous simulations of hydrocarbon hydrogenation reactions conducted without accounting for adsorbate surface diffusion. In the second part of the paper, we consider the extent to which the kinetics of reactions occurring on small metal particles are influenced by reactant adsorption on the support and reactant supply from the support. As an example, we discuss the kinetics of the CO oxidation reaction.

Keywords: Monte Carlo simulation; Model catalysts; ethylene hydrogenation; Carbon monoxide oxidation

1. Introduction

The microkinetic approach to modeling the kinetics of heterogeneous reactions, based on the use of mean-field kinetic models, has provided valuable insights into the mechanisms of a number of heterogeneous catalytic reactions [1]. The extent to which mean-field models can accurately predict the kinetics of a reaction occurring on a supported metal catalyst surface is, however, limited as mean-field models can only provide an approximate discription of the geometry or topology of the catalyst surface.

In order to account quantitatively for the effects of particle size in kinetic models, the activity or selectivity characteristics of supported metal catalysts are commonly correlated with the structural properties of ideal metal crystallites. However, particle size does not often correlate well with either catalytic activity or selectivity [2,3]. It is well known that the kinetics of a reaction can depend on the crystal face on which the reaction occurs [4], however, the overall rate of reaction cannot necessarily be estimated from the arithmetic average of the reaction rate on each facet due to communication between adjacent facets. If the reaction rate differs on the different facets of a supported metal particle then coupling of the reactions occurring on the difference facets can give rise to new kinetic phenomena [5]. It has also been shown that the structure of the metal particles, and therefore the reaction kinetics, may depend on the reaction conditions. Changes in the particle shape during the course of a reaction, induced by adsorption of the reactants, can also give rise to kinetic behaviour that cannot be accounted for by kinetic models based on the structure of

* Tel.: +44-131-650-4860

0920-5861/99/$ – see front matter
PII: S0920-5861(99)00122-4

ideal metal crystallites. Recent work on the methanol synthesis reaction by Ovesen et al. on particle restructuring [6] has led to the development of a microkinetic model for methanol synthesis that incorporates the dynamic restructuring of the metal particles during reaction.

The kinetics of a catalytic reaction need not only depend on the crystal structure of the metal particles for novel kinetic behaviour to be observed. As will now be discussed, for reactions where adsorbate spillover and the formation of ordered adsorbate domains occur, neither the crystal structure nor the electronic properties of the metal crystallites need necessarily influence the reaction kinetics for the reaction rate to be a function of metal particle size. In order to develop improved kinetic models of catalytic reactions occurring on supported metal catalysts, it is therefore necessary to account explicitly for the structure of the catalyst surface and for the physical and chemical processes that occur on the catalyst support.

The rate of adsorbate spillover onto the catalyst support from the dispersed metal particles and the corresponding rate of reverse-spillover can also depend on both the size and shape of the metal particles [7]. Adsorbate spillover and reverse-spillover can constitute critical steps of a catalytic cycle [8] and, in consequence, the kinetics of a catalytic reaction may be determined by the geometric properties of the metal particles. The adsorbate flux between the support and the metal particles can also depend on the spatial distribution of the metal particles on the catalyst support if neighbouring metal particles are sufficiently close together [9–12]. The influence of the spatial distribution of the metal particles on the support has been illustrated by the oxidation of CO by a model Pd/MgO catalyst [13]. As CO is capable of adsorbing on both the Pd particles and the MgO support the rate of reaction can be limited by the rate of supply of CO from the support to the metal particles where the oxidation reaction occurs. As neighbouring metal particles compete for the available CO molecules adsorbed on the support, the rate of CO oxidation becomes a function of particle separation as the metal particle density increases.

The rate of a catalytic reaction can also depend upon metal particle size due to the formation of an ordered adsorbate adlayer [11,12,14,15]. The formation of ordered adlayers can arise as a consequence of either surface diffusion limiting the rate of the surface reaction [16] or as a consequence of lateral interactions between the adsorbate molecules [17,18]. If the characteristic length of the adsorbate adlayer is comparable to the size of the dispersed metal particles then the structure of the adsorbate adlayer, and as a result the kinetics of the surface reaction, will be strongly influenced by the metal particle size and geometry [19,20].

Development of kinetic models that account for the structure of the catalyst surface is further motivated by recent progress in the synthesis of model catalysts that possess well defined geometric and topological properties. It is now possible, for example, to prepare model supported metal catalysts by electron-beam lithography [21,22] and by vapour deposition of metals on oxide supports [23]. An emerging area of catalyst synthesis of particular practical interest is the ordering of organometallic clusters within mesoporous silicas [24]. The ability to produce supported metal catalysts consisting of regularly arranged metal particles with a narrow size distribution, without recourse to elaborate lithographic or vapour deposition technologies, is a prerequisite for the industrial application of supported metal catalysts with well defined structural properties.

In this paper, we present the results of Monte Carlo studies of two heterogeneous reactions occurring on the surface of a highly dispersed supported metal catalyst. First, we consider the influence of metal particle size and geometry on the kinetics of a model hydrocarbon hydrogenation reaction. It has been demonstrated previously that, in the absence of adsorbate surface diffusion, metal particle shape does not influence the kinetics of hydrocarbon hydrogenation reactions to a significant extent [25]. In this case, the reaction kinetics can be approximated by a modified ensemble model that accounts only for variations in the metal particle size. An immobile adsorbed adlayer cannot be assumed, however, for reactions where rapidly diffusing hydrogen species are present on the catalyst surface. In the first part of this paper, therefore, we extend previous Monte Carlo studies of hydrocarbon hydrogenation reactions to consider the influence of metal particle size and geometry on the kinetics of a hydrogenation reaction in which hydrogen is assumed to diffuse on the catalyst surface.

In the second part of this paper, we present the results of a Monte Carlo study of the CO oxidation

reaction on small metal particles where the adsorption and diffusion of CO on the catalyst support occurs. We discuss the extent to which mean-field models of reaction and surface diffusion based on simplified models of the surface geometry can be expected to apply to the disordered surfaces structures that are representative of supported-metal catalysts.

2. Hydrocarbon hydrogenation reactions on highly dispersed catalysts

2.1. Methodology

We have undertaken Monte Carlo (MC) simulations of a series hydrocarbon hydrogenation reactions in order to determine the activity of a series of model catalyst surfaces representative of highly dispersed supported metal materials. MC simulations have provided insights into the mechanisms of a number of important catalytic reactions, including CO oxidation [26] and the hydrogenation of short-chain alkenes [27,28]. Microkinetic models of catalytic reactions typically assume that the reaction occurs on a surface that is both homogeneous and infinite in extent. In supported metal catalysis, however, the reaction does not occur on an infinite surface but, rather, in a confined geometry that is defined by the boundaries of the dispersed metal particles. In the case of highly dispersed supported metal catalysts, the characteristic length of the region to which the reactants are confined can be equivalent to only a few adsorbate molecule diameters. Previous studies of catalytic reactions occurring in confined geometries have demonstrated that there are significant differences between the kinetics of a reaction that occurs on an infinite surface and one that occurs within a confined geometry [5,20,29]. Detailed simulations of a catalytic reaction are therefore required if the geometric structure of the metal particles or the topology of the catalyst surface are suspected to influence the reaction kinetics.

While MC simulations have been used extensively to model the kinetics of simple reactions on single crystal surfaces [30], their use in applied catalysis has been limited by the complexity of the catalytic processes that occur on the surface of supported metal catalysts. Simulating complex reaction mechanisms, in particular where surface diffusion is included, can be place excessive demands on computing resources. MC simulations of catalytic reactions on small particles have been used previously in order to account for kinetic behaviour observed for the hydrogenation of ethylene by Pt/silica catalysts [15] and the oxidation of CO by Pd/SnO_2 [31]. In this section, we extend our recent work on the simulation of reactions on supported metal catalysts to consider the influence of metal particle size, surface diffusion, and adsorbate spillover on a reaction mechanism representative of a hydrocarbon hydrogenation reaction.

We consider a model hydrogenation reaction between a rapidly diffusing species representing a hydrogen atom, A, and an immobile polyatomic molecule B_n, representing the hydrocarbon. The mechanism for this reaction can be simplified to

$$A + * \rightleftarrows A^* \quad (1)$$

$$B_n + n* \rightarrow B_n^* \quad (2)$$

$$A^* + B_n^* \rightarrow 2^* \quad (3)$$

where the superscript * denotes a molecule that is adsorbed on the catalyst surface.

This simplified two-step mechanism is a reasonable approximation for describing the hydrogenation of hydrocarbons [32] and has been studied previously in the absence of surface diffusion or adsorbate spillover [25]. The adsorption of the hydrocarbon molecule is described by the path of random walk that occupies n lattice locations on the catalyst surface. The surface reaction is assumed to follow a Langmuir–Hinshelwood mechanism in which the product molecules desorb rapidly and irreversibly from the catalyst surface. The rate of the surface reaction is assumed to be infinite and reaction immediately occurs between neighbouring A and B_n species.

A MC algorithm for the efficient simulation of reactions with rapid surface reaction and A diffusion was introduced by Zhdanov and Kasemo for the $A+B_2 \rightarrow 0$ reaction in order to study the oxidation of CO and H_2 by supported metal particles [11,12]. In this study, it was argued that under conditions where one of the reactants diffuses rapidly on the catalyst surface only the distribution of the other, immobile, reactant need be accounted for. If it is assumed that the A atoms (hydrogen atoms) diffuse rapidly on the metal particles then every A atom will react with a B_n molecule

(hydrocarbon molecule) before the next A adsorbs at the catalyst surface. If it is further assumed that the B_n molecules are immobile, then the A and B_n species cannot co-exist on the surface of the metal particles. We need therefore only explicitly account for the distribution of the strongly adsorbed B_n molecules on the surface. In this paper, we extend the previous study of the $A + B_2 \rightarrow 0$ reaction with A diffusion on a homogeneous surface to consider the general case of the $A + B_n \rightarrow 0$ reaction occurring on disordered surfaces.

We now consider the application of the simulation algorithm discussed above to a specific reaction mechanism and, in particular, argue that the simulation algorithm provides an appropriate description of a hydrocarbon hydrogenation mechanism under typical conditions corresponding to reaction at atmospheric pressure and a temperature of 300 K. We consider data obtained from a microkinetic analysis of the hydrogenation of ethylene by silica supported platinum [33,34]. For ethylene hydrogenation at temperatures below 300 K the catalyst surface is saturated by a strongly adsorbed hydrocarbon layer, the active species most likely being π-bonded ethylene [35]. It is further assumed that the hydrocarbon is strongly adsorbed and immobile on the catalyst surface. The assumption that the adsorbed reactants are immobile, while reasonable for a strongly adsorbed hydrocarbon adlayer, is unlikely to apply in the case of hydrogen as the activation barrier for surface diffusion is very low. The activation energy for the diffusion of hydrogen on platinum for example is only $\approx 10\,\mathrm{kJ\,mol^{-1}}$. Furthermore, at all but very low temperatures the rate of the surface hydrogenation reaction is also very rapid [34]. Thus, as the rate of diffusion of dissociated hydrogen and of the surface reaction are expected to be far greater that the rate of desorption of the hydrocarbon, the efficent MC algorithm discribed above can be applied to the hydorgenation mechanism described above.

At low temperatures, and at high hydrocarbon pressures, the catalyst surface is saturated by the adsorbed hydrocarbon adlayer. Under these conditions small molecules, in particular hydrogen, can adsorb non-competitively on the vacant lattice sites in the hydrocarbon layer that cannot be occupied by the larger hydrocarbon molecules. At higher temperatures, or lower hydrocarbon pressures, the reactants compete for the available adsorption sites on a surface largely free of reactive hydrocarbon molecules. The presence of distinct adsorption sites for the hydrocarbon and hydrogen species has been proposed previously in order to explain the temperature dependence of the reaction orders in hydrogen that are observed experimentally for the hydrogenation of ethylene [33,34]. The rate limiting step, and therefore the kinetic orders with respect to each reactant, have been shown to differ for hydrocarbon covered and hydrocarbon free surface [27]. The nature of the transition between the kinetic regimes that correspond to the hydrocarbon covered and hydrocarbon free surface has been discussed in detail previously with respect to the hydrogenation of short-chain alkenes [28].

The reaction mechanism as given by Eqs. (1)–(3) clearly represents a simplification of an actual hydrocarbon conversion reaction for which undesirable side reactions will be present. Under typical reaction conditions, the majority of the catalyst surface will be covered by carbonaceous deposits of some form. Infrared studies of the surface reaction suggest, however, that the reaction occurs on the few regions of the catalyst surface that are not covered by these inactive deposits [35]. Therefore, although the surface is mainly covered by an carbonaceous overlayer, the presence of coke or an inactive hydrocarbon species only reduces the total area available for reaction and does not influence the reaction mechanism.

2.2. Simulation algorithm

The theoretical background to MC simulation techniques and to their application in heterogeneous catalysis has been the subject of previous review articles [30,36,37] and therefore will not be discussed in detail here. In the MC method, the physical and chemical processes constituting the steps of the reaction mechanism are represented by a series of discrete transformations of a simulation lattice that is representative of the catalyst surface. The simulation lattice is assumed to consist of N discrete adsorption sites, each of which can either be vacant or be occupied by an adsorbate molecule.

The lattice on which the reaction simulation is conducted has been constructed to reproduce the disordered surface of a supported metal catalyst. Specifically, the simulation lattice is produced by first

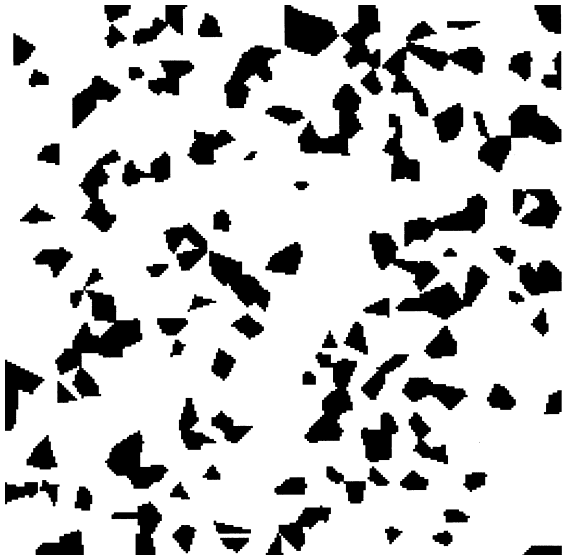

Fig. 1. An example simulation lattice generated by a Voronoi tessellation of the plane with $\phi = 0.5$. Black regions represented the dispersed metal particles and white regions the catalyst support.

generating a Voronoi tessellation of the plane [38] which divides the plane into a large number of irregular polygons. Each of these polygons, which is in turn composed of a number of discrete adsorption sites, is designated as representing either a metal particle or a region of the catalyst support. As the number fraction, ϕ, of the polygons that are assigned to represent the metal particles increases, the average size of the metal particles also increases due to the coalescence of neighbouring polygons. The lattices produced by this algorithm are intended to represent a projection of the catalyst surface onto the plane and look similar to the images of supported metal catalysts that are obtained from electron microscopy [39]. A representative simulation lattice, for which $\phi = 0.5$, is shown in Fig. 1. In the present study we consider only regular square lattices of side length $\sqrt{N}$. The use of lattices of other co-ordination numbers is a trivial extension of the work described here. A discussion on the application of the Voronoi tessellation in supported metal catalysis has been presented previously [25].

The reactant molecules are assumed to rain down on to the catalyst surface from an infinite reservoir representing the bulk gas phase. Molecules adsorb onto the surface subject to a number of rules that define the reaction mechanism described in the previous section. An efficient MC simulation algorithm to simulate the $A + B_n \rightarrow 0$ reaction occurring on the metal particles without adsorption on the metal support or adsorbate spillover is detailed below.

1. *Site selection.* The simulation begins by selecting one of the two possible reactants. An A being selected with a probability Pr_A. As inert components are assumed to be absent from the reactant mixture, the probability of a B_n molecule being selected is given by $Pr_B = 1 - Pr_A$. An adsorption site on the lattice is then chosen at random. If the chosen lattice location is a vacant site on a metal particle then an attempt is made to adsorb the molecule (Step 2). The adsorption attempt fails if the site is occupied by another molecule, or is an adsorption site on the metal support.
2. *Adsorption.* If the chosen species is an A then an A adsorbs successfully on the vacant site, occupying a single site on the metal particle. If a B_n molecule is selected then an attempt is made to complete a random walk occupying n sites on the metal particle. If the random walk can be completed, without the molecule encountering the particle boundary or another adsorbed molecule, then the B_n molecule adsorbs, occupying the n lattice sites.
3. *Reaction.* If an A molecule adsorbs on a site that is adjacent to any previously adsorbed B_n molecules then a neighboring B_n molecule is selected at random and both of the reactant molecules immediately desorb from the surface.
4. *Diffusion.* If the adsorbed molecule is an A, and no immediate B_n neighbours are found after adsorption, then the molecule is allowed to diffuse within the boundaries of the metal particle until a B_n molecule is found. A reaction then occurs and both reactants are removed from the surface. The B_n molecule is assumed to be immobile and cannot diffuse on the surface. The adsorption of A is assumed to be rapid and reversible. Therefore, if no B_n molecules are found on the particle A then desorbs from the particle.

Each simulation was run for a sufficient number of adsorption attempts for steady state to be attained. The turnover number of the reaction, R, is defined by

$$R = \frac{N_r}{tN\Phi} \tag{4}$$

where N_r is the number of reactions occurring in t MC steps (MCS), where a single MCS represents 256×256 adsorption attempts, and Φ the fraction of the total number of adsorption sites that lie within the boundaries of the metal particles.

The least efficient step of the algorithm is Step 4, the diffusion of the A atom. At low B_n coverage the time taken to simulate the random walk of the A atom before it locates an adsorbed B_n molecule can become excessive and longer simulations become impractical. It is, however, unnecessary to conduct random walks at low B_n coverage. As the distribution of B_n on the metal particles is uncorrelated at low surface coverage, the mean-field approximation applies and the diffusion and reaction step need not be explicitly simulated by a time consuming random walk. If θ_B^j denotes the B_n coverage on a specific metal particle j, then for $\theta_B^j < \theta_B^*$ an A random walk is not conducted on that particle. The value of θ_B^* is defined to be low enough to ensure the mean-field approximation holds. For $\theta_B^j < \theta_B^*$, a randomly selected B_n molecule is chosen from the metal particle and both reactants are then removed from the particle. In practice it is found that for $\theta_B^* \leq 0.05$ the reaction rates obtained using the more efficient algorithm were identical, within the accuracy of the simulations, to those obtained using the random walk algorithm.

Simulations were conducted on a square lattices of 256×256 adsorption sites. Approximately 10^4 MCS were used to obtain a reliable estimate of the reaction turnover number. Each simulation was repeated on 50 randomly generated tessellations with the same number density of Voronoi polygons assigned as metal particles.

2.3. An ensemble model for reactions on dispersed metal catalysts

We first discuss the basic simulation algorithm described above and neglect any form of interaction of the reactants with the support. In order to relate the structure of the catalyst surface to its catalytic characteristics we consider the important parameter to be not the absolute metal particle size, but rather the relative size of the B_n molecules and the metal particles. Let the radius of a metal particle, j, be denoted by l_j. The radius for each particle is then defined as the average distance between each lattice location within a metal particle and the particle edge,

$$l_j = |d_k|, \tag{5}$$

where d_k is the radial distance between an adsorption site, k, on a metal particle and the particle boundary. The radius of each particle is calculated from the average of a series of particle radii separated by 45°. The corresponding average particle radius, l, is then obtained by taking the average of l_j over all the metal particles on the catalyst surface. The average dimensionless particle radius for a given reaction on a particular surface can then be defined by

$$\langle l \rangle = \frac{l}{n}. \tag{6}$$

where n is the length of the B_n molecule representing the hydrocarbon chain.

For a disordered surface, as is constructed from the Voronoi tessellation, the particle radius and the corresponding dimensionless particle radius must be calculated numerically for each surface. However, for a surface composed only of square particles of side length L the value of $\langle l \rangle$ can be computed exactly where,

$$\langle l \rangle = \frac{1}{4Ln} \int_0^L (L + \sqrt{2}x)\, \mathrm{d}x \tag{7}$$

which integrates to

$$\langle l \rangle = \frac{1 + 1/\sqrt{2}}{4n} L. \tag{8}$$

As a measure of the activity of the catalyst surface, R, we introduce the surface effectiveness factor, η, defined as the ratio of the measured reaction rate on a disordered surface to the corresponding reaction rate under the same conditions on a homogeneous surface, R^*, where

$$\eta = \frac{R}{R^*}. \tag{9}$$

As the particle radius for a square can be obtained from Eq. (8), an expression for the effectiveness factor of a surface consisting of a regular tiling of square metal particles can be derived from the ensemble theory [40]. For a mean particle radius, $\langle l \rangle$, the effectiveness factor for a surface composed of square particles is given by [25]

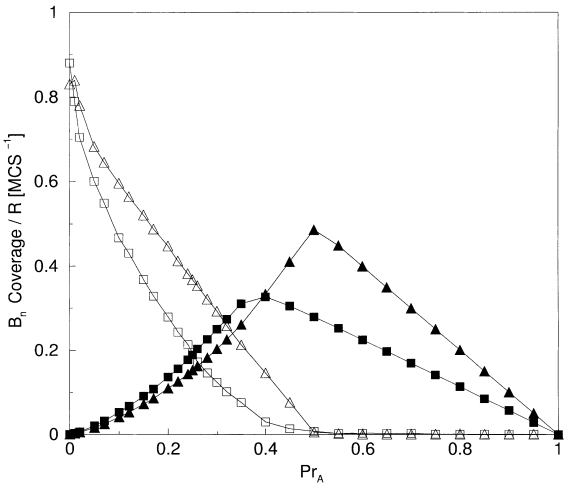

Fig. 2. The turnover number of the $A + B_5 \rightarrow 0$ reaction and the corresponding surface coverage of the B_5 molecules for a homogeneous surface (△) and Voronoi tessellation with $\phi = 0.5$ (□) Empty symbols correspond to the B_5 coverage and filled symbols to the reaction rate.

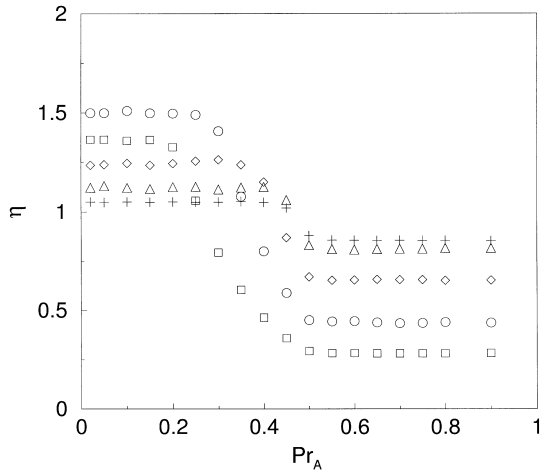

Fig. 3. The effectiveness factor as a function of $\langle l \rangle$ for the $A + B_n \rightarrow 0$ reaction in the absence of A spillover. Data are shown for $\langle l \rangle$ values of 1.16 (□), 1.26 (○), 2.17 (◇), 4.08 (△), and 4.67 (+).

$$\eta = \frac{(4/(1 + 1/\sqrt{2})\langle l \rangle - 1)^2}{(4/(1 + 1/\sqrt{2})\langle l \rangle)^2}. \tag{10}$$

If the activity of a catalyst surface were to be determined by the size of the metal particles alone, and not by the geometry of the particles or the topology of the surface, we would expect that the effectiveness factor obtained from the simulation of a reaction on a disordered surface to agree with the analytical solution obtained from a regular surface composed of an array of square metal particles.

2.4. Results

In Fig. 2 the results of MC simulations of the $A + B_5 \rightarrow 0$ reaction are presented. The reaction turnover number and the corresponding surface coverage of the B_n molecules are shown as a function of Pr_A for both a homogeneous surface ($\phi = 1.0$), and for a disordered surface ($\phi = 0.5$). Two distinct kinetic regimes can be identified. At low values of Pr_A the catalyst surface is covered by a strongly adsorbed adlayer of B_n molecules and the reaction rate is determined by the rate at which the A molecules can adsorb in the interstices that exist within the B_n adlayer. As Pr_A increases, there is a continuous transition from a B_n saturated surface to a surface that is largely free of adsorbate molecules. For a homogeneous surface, B_n molecules cannot exist on the catalyst surface for $Pr_A > 0.5$ due to the rapid diffusion of A. For a disordered surface, consisting of a distribution of metal particles the transition from the B_n covered regime will occur at lower values of Pr_A due to inhibition of the adsorption of the large B_n molecules on the small metal particles.

The effectiveness factors obtained from MC simulations of the $A + B_n \rightarrow 0$ reaction are shown in Fig. 3 as a function of Pr_A with the dimensionless particle radius $\langle l \rangle$ given as the parameter. For $Pr_A > 0.5$, the reaction rate is limited by the rate of adsorption of the larger B_n molecules onto the metal particles. In this kinetic regime, the total adsorbate surface coverage is negligible and the effectiveness factor is therefore independent of Pr_A. As the total adsorbate coverage is negligible, it can be expected that the ensemble model will apply in this regime as the characteristic length of the adsorbate free regions onto which the B_n molecules adsorb will be defined by the metal particle boundaries.

Fig. 4 shows a plot of the effectiveness factors for $Pr_A = 0.8$ predicted by Eq. (10) compared with the results of a series of MC simulations. Simulations were conducted on surfaces generated from Voronoi tessel-

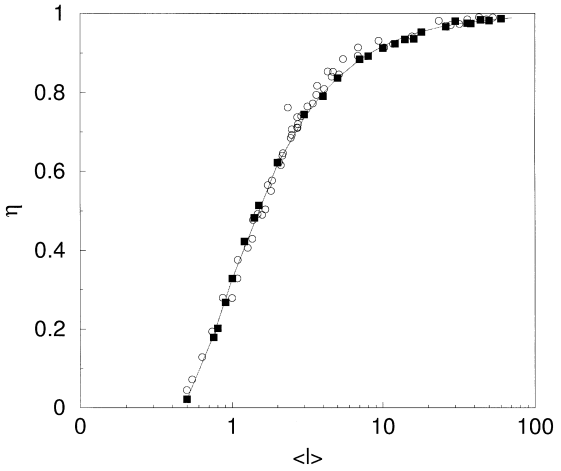

Fig. 4. The effectiveness factor for reaction for the $A + B_n \rightarrow 0$ reaction in the absence of A spillover for the low surface coverage regime ($Pr_A = 0.8$). Data are shown for a Voronoi tessellation (○) and a for surface composed of a tiling of rectangles (■). The effectiveness factor predicted by Eq. (10) is shown as the solid line.

lations of the plane (circles) and from a tiling of regular square islands (squares). Data are shown as a function of the dimensionless particle diameter $\langle l \rangle$ for a series of randomly selected surfaces ($0.05 \leq \phi \leq 0.95$) and B_n molecule sizes ($2 \leq n \leq 20$). The solid line corresponds to the predictions of the ensemble model. For reaction on a disordered catalyst surface, the effectiveness factor is found to be a function only of the dimensionless particle length. This result, that the reaction rate depends only on the particle size and is independent of the particle shape, is confirmed by a further set of MC simulations conducted on surfaces consisting of arrays of square metal islands. Agreement is obtained between the results of the simulations conducted on the Voronoi tessellations and on the tiling of squares. The results obtained for reaction with rapid A diffusion are found to be in agreement with simulations conducted previously for the case of immobile reactants [25]. In this case the effectiveness factor was also found to depend only on the dimensionless particle size.

For $Pr_A \ll 0.5$, the catalyst surface is covered with an adlayer of adsorbed B_n molecules and the rate of reaction will be determined by the rate of A adsorption. For $Pr_A \ll 0.5$, the activity of the disordered surface for a given reactant composition is found to be greater than that on a homogeneous surface. The increased activity of the disordered surface is a consequence of the reduced rate of B_n adsorption on small metal particles. Reducing the size of the metal particles allows for non-competitive adsorption of A at the particle boundaries where the adsorption of B_n is sterically hindered. Therefore, as the metal particle size declines the number of vacant sites available for adsorption of A increases and the reaction rate increases accordingly. As the catalyst surface consists of a distribution of particles sizes, there is a continuous rather than discontinuous transition from the regime for which $\eta < 1$ and for which $\eta > 1$.

We now briefly consider the case where adsorbate spillover onto the catalyst support can occur. The MC algorithm is assumed to be identical to that described previously for the $A + B_n \rightarrow 0$ reaction with the exception that A is now allowed to diffuse across the metal particle-support boundary. Spillover of A is simulated, as previously, by conducting a random walk on the simulation lattice. The effectiveness factors obtained by including A spillover are presented in Fig. 5. As can be seen by comparison with the data obtained in the absence of A spillover the effectiveness factors obtained are identical, to within the accuracy of the simulations, for both kinetic regimes. This result can be explained as follows. In the high B_n coverage regime, A immediately reacts on adsorption before it can spillover onto the support, the rate of spillover

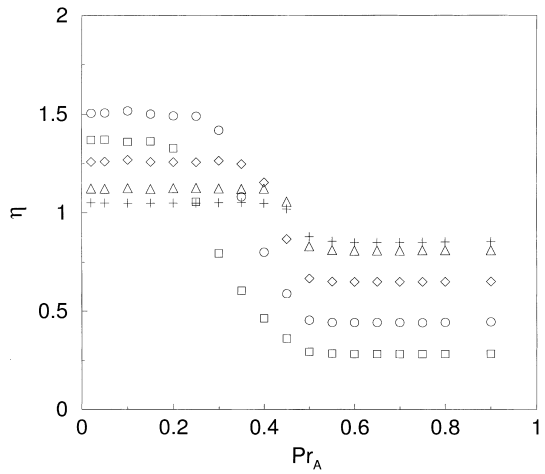

Fig. 5. The effectiveness factor as a function of $\langle l \rangle$ for the $A + B_n \rightarrow 0$ reaction with A spillover onto the support. Data are shown for $\langle l \rangle$ values of 1.16 (□), 1.26 (○), 2.17 (◇), 4.08 (△), and 4.67 (+).

to the support is therefore negligible. In the low surface coverage regime, spillover of A molecules does not influence the reaction rate as the reaction rate is determined only by the rate of adsorption of the B_n molecules.

In summary, a Monte Carlo model for hydrocarbon hydrogenation reactions accounting for the rapid diffusion of hydrogen on highly dispersed supported-metal particles has been discussed. It has been shown that the reaction kinetics are independent of the geometry of the metal particles and depend only on the relative sizes of the hydrocarbon molecules and the metal particles. In agreement with previous simulations of hydrogenation reactions without surface diffusion we find the reaction kinetics can be accurately described by an ensemble model.

3. Reaction with reactant supply from the support

3.1. A mean-field model for reaction with reactant supply from the support

If adsorption of one of the reactants occurs on the catalyst support then, in addition to direct adsorption on the metal particles, reactant molecules can reach the dispersed metal particles by diffusion of the adsorbed molecules across the support to the support-particle boundary. Reactant supply from the support has been shown to be important in a number of catalytic processes [23] including reversible oxygen storage in Pd/Ceria oxidation catalysis, the reverse spillover of hydrogen from hydroxylated oxide supports, and the adsorption and diffusion of CO on oxide supports. The adsorption and diffusion of CO on refractory oxides has been studied extensively and will therefore be the focus of this discussion.

Within a limited range of reaction conditions, the rate of CO oxidation catalysed by oxide supported Rh particles has been shown to be determined by the rate of diffusion of CO adsorbed on the catalyst support [41,43]. Studies of CO oxidation catalysed by a number of oxide supports including mica [42] and α-alumina [41,43] have demonstrated that the reaction rate can depend on the density of the metal particles distributed on the support. This result can be explained if it is assumed that the rate limiting step is the transport of reactant molecules from the support to the metal particles.

If the rate of oxidation of CO on the metal particles is more rapid than the rate of diffusion of the CO adsorbed on the support, then the CO coverage on the support will be a function of the radial distance from each particle. Each particle will therefore be surrounded by a depleted zone within which the CO coverage is reduced with respect to the bulk of the support due to reaction at the metal particle boundary. As the number density of metal particles on the surface increases, the areas of reduced CO coverage surrounding each particle eventually overlap. Overlap of the depleted zones will reduce the adsorbate supply from the support, leading to a reduction in the reaction rate. The width of the depleted region surrounding each individual particle is determined by the diffusion length, l_d, of the CO molecule adsorbed on the oxide support. The diffusion length, the distance an adsorbed molecule can diffuse before it desorbs from the support surface, can be defined in terms of the surface diffusion coefficient, D, and the rate of desorption from the support, κ_{des}, where

$$l_d = \sqrt{\frac{D}{\kappa_{des}}}. \tag{11}$$

A kinetic model incorporating support adsorption and diffusion was first proposed for describing nucleation kinetics and particle growth [44]. This model was later extended to account for the enhanced sticking probability of CO on Pd/mica [42]. The basic model can be summarised as follows. Perfectly circular metal particles, of radius r_o, are distributed uniformly on the catalyst support. Each metal particle is surrounded by a region of the catalyst support that is depleted of adsorbed CO that extends to a distance L from the centre of the metal particle. Molecules of CO that adsorb on the catalyst support migrate toward the metal particle driven by a radial concentration gradient. The metal particles are assumed to be separated by a distance large enough to ensure that the depleted zones do not overlap. The concentration profile of the adsorbate within the depleted region, $\Theta(r)$, is given by the solution of the diffusion equation

$$\frac{\partial\Theta(r,t)}{\partial t} = \alpha\kappa_{ads} + D\left[\frac{\partial^2\Theta(r,t)}{\partial r^2} + \frac{1}{r}\frac{\partial\Theta(r,t)}{\partial r}\right] - \kappa_{des}\Theta(r,t), \tag{12}$$

where κ_{ads} is the rate of adsorption on the catalyst support and α the sticking coefficient.

Analytical solutions to the diffusion equation can be obtained only if it is assumed that the metal particles are of uniform shape and size. For the CO oxidation reaction, the following boundary conditions were proposed by Henry et al. [43]. (i) Reaction on the metal particles is assumed to be a rapid process, the metal particles therefore act as a set of perfect sinks and $\Theta(r_o) = 0$. (ii) It is assumed that the particles are widely separated, therefore there is no net flux across the boundaries of the depleted regions and so $\partial\Theta/\partial r = 0$ at $r = L$. The CO concentration profile at steady state corresponding to these boundary conditions is given by [44]

$$\Theta(r) = \frac{\alpha\kappa_{ads}}{\kappa_{des}} \times \left[1 - \frac{I_0(r/\delta)K_1(L/\delta) + I_1(L/\delta)K_0(r/\delta)}{I_0(r_o/\delta)K_1(L/\delta) + I_1(L/\delta)K_0(r_o/\delta)}\right], \quad (13)$$

where I_i and K_i denote the ith order modified Bessel functions. These boundary conditions will only apply if the transport of CO across the particle boundary is irreversible. This will be the case if the metal particles are covered by adsorbed oxygen ($Pr_{CO} < 0.525$) or if the rate of CO desorption from the support is rapid. Both this assumptions are implicit in the Monte Carlo model considered in this work. For situations where the particles are covered with CO, the boundary conditions should be modified such that the adsorbate flux is equated to the overall reaction rate [11,12].

Eq. (13) has been successfully applied to model catalyst surfaces with well defined particle size distributions [45]. The present work will consider the extent to which the diffusion model can be applied to catalyst surfaces where the metal particles are not circular and where the metal particle size is more accurately described by a particle size distribution. To this end, MC simulations have been conducted for catalyst surfaces consisting of circular islands and for surfaces described by Voronoi tessellations. The results of the numerical simulations are then compared to the analytical solution of Eq. (13) incorporating a particle size distribution.

3.2. Model and algorithm

The CO oxidation reaction is assumed to progress via the single step Langmuir–Hinshelwood mechanism

$$CO + * \rightleftarrows CO^* \quad (14)$$

$$O_2 + 2^* \rightarrow 2O^* \quad (15)$$

$$CO^* + O^* \rightarrow 2^* \quad (16)$$

where the superscript * denotes an adsorbed species.

The oxidation of CO has been the subject of several previous MC studies assuming immobile reactants [26], this assumption is only realistic at low reaction temperatures however. Zhdanov and Kasemo recently introduced a MC algorithm for CO oxidation incorporating CO diffusion [11,12]. It was argued that as the rate of the surface reaction is rapid compared to the rate of CO diffusion, which is in turn rapid compared to the rate of oxygen diffusion, an efficient MC algorithm could be used to account for the diffusion of CO on the catalyst surface. The algorithm for implementing the CO oxidation mechanism with CO diffusion is therefore similar to that described previously for hydrocarbon hydrogenation with the exception that CO is permitted to both adsorb and diffuse on the catalyst support.

1. *Site selection.* The simulation begins by selecting a lattice location on the support. If the selected site is vacant then an attempt is made to adsorb either a CO or O_2 molecule. Adsorption of CO can occur on both the metal particles and the support. Adsorption of O_2 can occur only on the metal particles. In the simulation results reported here the probabilities of CO and O adsorption are assumed to be equal.
2. *Diffusion on the support.* If a CO molecule adsorbed on the support is selected it may either desorb from the support or diffuse across the support. The probability of a desorption event occurring is given by ratio of the rates of diffusion and desorption, $\kappa_{dif}/\kappa_{des}$. Diffusion of CO is simulated by conducting a random walk on the support. On reaching the particle boundary the CO molecule obeys the same rules as if it had adsorbed at that location on the metal particle.

3. *Reaction on metal particles.* If a CO molecule adsorbs on a site that is adjacent to any O* species, one of the neighboring adsorbed O atoms are selected at random and both of the reactant molecules immediately desorb from the surface.
4. *Diffusion on metal particles.* If the adsorbed molecule is a CO, and no immediate O neighbours are found after adsorption, the molecule is allowed to diffuse within the boundaries of the metal particle until an O is found. If an adsorbed O is found, a reaction then occurs and both reactants are removed from the lattice. If there are no O atoms on the metal particle the CO molecule is assumed to desorb from the particle, this criterion ensures the boundary condition $\Theta(r_o) = 0$ is satisfied.

The only additional parameter required for simulation of adsorption and diffusion on the support is the desorption probability $\kappa_{dif}/\kappa_{des}$ that defines the diffusion length of CO on the catalyst support. Assuming that both desorption from the catalyst support and diffusion across the support are activated processes, the relative rates of diffusion and desorption are given by

$$\frac{\kappa_{dif}}{\kappa_{des}} = \exp\left[\frac{(E_{des} - E_{dif})}{k_b T}\right], \quad (17)$$

where E_{des} and E_{dif} are the respective activation energies for desorption from the support and diffusion on the support. The corresponding diffusion length is given by

$$l_d = a\exp\left[\frac{(E_{des} - E_{dif})}{2k_b T}\right], \quad (18)$$

where a is the jump length of a CO molecule adsorbed on the support.

Using data obtained for the diffusion of CO on α-alumina, $E_{des} - E_{dif} = 18.8\,\text{kJ mol}^{-1}$ [45]. At a typical reaction temperature of 390 K, a diffusion probability of $\kappa_{des}/\kappa_{dif} \approx 18.8$ and a diffusion length of $l_d \approx 5$ nm on Pd, is obtained assuming a jump length of $a = 0.23$ nm. Calculating the diffusion length from Eq. (17) will, however, overestimate the actual diffusion length for two reasons. First, Eq. (17) only applies strictly in the limit of low surface coverage as the diffusion length will be independent of Θ only as $\Theta \to 0$. Second, Eq. (17) assumes isotropic diffusion perpendicular to the particle radius. A more accurate measure of the diffusion length can be calculated numerically from the mean square displacement of the molecules within the capture radius where $a\exp[(E_{des} - E_{dif})/2k_b T]$ will represent the upper bound on the diffusion length.

3.3. Simulation results

Concentration profiles have been obtained by MC simulation for surfaces of a regular geometry (circular islands) and for surfaces represented by a Voronoi tessellation of the plane. Simulations were conducted for two values of $\kappa_{dif}/\kappa_{des}$ corresponding to reaction at 390 K ($\kappa_{dif}/\kappa_{des} = 20$) and 300 K ($\kappa_{dif}/\kappa_{des} = 50$). The diffusion lengths calculated from the RMS displacement of the CO molecules on the support under these conditions were 2.2 and 3.8, respectively. The unit length being defined as the side length of each adsorption site. Using the calculated values of the diffusion lengths, a comparison between the analytical solution of the diffusion equation with and the results of the MC simulations was obtained for each set of reaction conditions.

In Fig. 6 the analytical solution to the diffusion equation is compared to the results obtained from the MC simulations of reaction occurring on circular islands of radius $r_o = 5$ using the diffusion lengths obtained from the simulations. For a catalyst surface

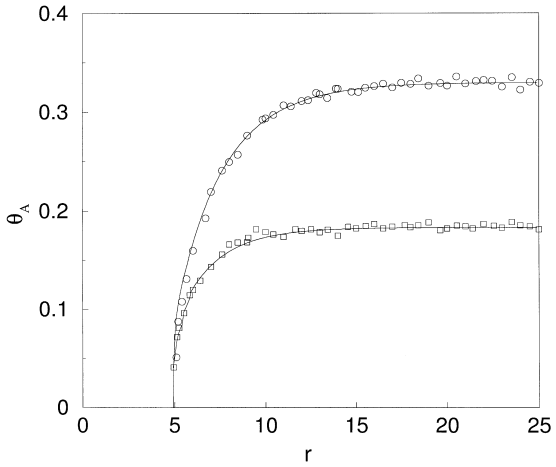

Fig. 6. Radial concentration profiles for CO adsorbed on the catalyst support, $\Theta(r)$, obtained by MC simulation and by the solution of Eq. (13) with $\kappa_{dif}/\kappa_{des} = 20$ (○) and $\kappa_{dif}/\kappa_{des} = 50$ (□). Data are shown for circular islands of radius $r_o = 5$.

composed only of circular islands, there is good agreement between the solution of the diffusion equation and the MC simulations as would be expected for widely separated islands of circular geometry.

In order to apply the mean-field analysis to supported metal catalysts, is necessary to investigate the extent to which Eq. (13) can be applied to a catalyst surface that consists of a distribution of particle sizes. Eq. (13) can be re-written to incorporate a distribution of particle sizes as

$$\Theta(r) = \int_0^\infty F(r_o)\frac{\alpha\kappa_{ads}}{\kappa_{des}} \times \left[1 - \frac{I_0(r/\delta)K_1(L/\delta) + I_1(L/\delta)K_0(r/\delta)}{I_0(r_o/\delta)K_1(L/\delta) + I_1(L/\delta)K_0(r_o/\delta)}\right] dr_o, \quad (19)$$

where $F(r_o)$ defines an appropriate particle size distribution for the Voronoi tessellation subject to the constraint

$$\int_0^\infty F(r_o)\, dr_o = 1. \quad (20)$$

The particle size distribution describing the tessellation can be obtained by calculating the equivalent radius of a circle with the same area as the polygonal region representing each metal-particle. For a Voronoi tessellation consisting of randomly distributed polygons, the distribution of particle sizes is expected to be described by Gaussian distribution. Fig. 7 presents the measured particle size distribution for a series of Voronoi tessellations, for which $\phi = 0.1$, and the corresponding best fit Gaussian distribution. This Gaussian function was used as the expression for $F(r_o)$ in Eq. (19).

The MC simulations were conducted using the same parameters as for the surface composed of circular islands. Simulations were run for 5×10^3 MCS and each simulation was repeated for 50 randomly generated lattices for which $\phi = 0.1$. For a highly dispersed supported metal catalyst surface a metal surface coverage of $\approx$0.1 is typical. A representative image of the simulation lattice showing the density of CO molecules on the support is shown in Fig. 8. The metal particles appear as the black regions and the regions of high CO density appear as the white regions.

In Fig. 9 the results of the MC simulations (circles) and the numerical integration of Eq. (19) incorporating the measured particle size distribution, are shown for the two values of $\kappa_{dif}/\kappa_{des}$. The results for a highly dispersed surface are found to be in good agreement with the numerical simulations. This result would suggest that Eq. (13) can be applied to distribution of particle sizes, provided the particle density on the

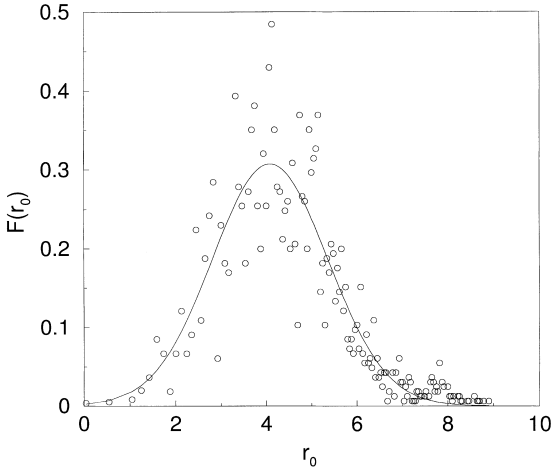

Fig. 7. The particle size distribution obtained from sampling 50 randomly generated Voronoi tessellations with $\phi = 0.1$. The best fit Gaussian function is shown as the solid line.

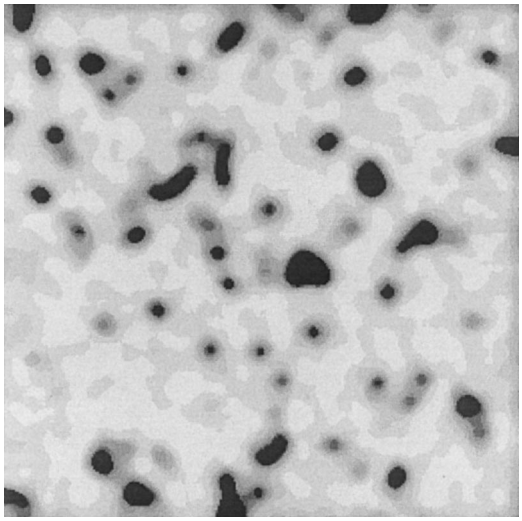

Fig. 8. A snapshot of the simulation lattice showing the distribution of CO adsorbed on the catalyst support. The white regions correspond to areas of high CO coverage (maximum =0.14) and dark regions to areas of low coverage. The metal particles are saturated with adsorbed O and therefore appear black.

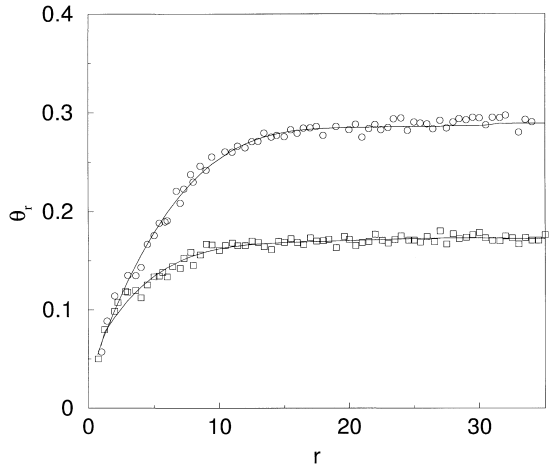

Fig. 9. Radial concentration profiles for CO adsorbed on the catalyst support, $\Theta(r)$, obtained by MC simulation of CO oxidation on a Voronoi tesselation and by the solution of Eq. (13) with $\kappa_{dif}/\kappa_{des} = 20$ (○) and $\kappa_{dif}/\kappa_{des} = 50$ (□). Data are shown for a Voronoi tessellation with $\phi = 0.1$.

support is low enough to ensure the depleted zones do not overlap.

We can conclude from the simulations of reaction and diffusion on the Voronoi tessellations that the diffusion equation for a disordered surface can be approximated by the solution obtained for circular islands with a Gaussian particle radius distribution. This result is a consequence of averaging the CO coverage profiles obtained for a large number of randomly oriented polygons. The CO distribution cannot be accurately approximated by an equivalent circular island for a single polygon as the CO concentration profile will not be symmetric about the centre of the particle, as is the case for a circular island. Averaging over a large number of randomly oriented polygons will, however, result in a symmetric CO concentration profile. For this reason, simulations conducted on a number of Voronoi tessellations are found to produce results that are in good agreement with the solution for the diffusion equation given by Eq. (13).

4. Summary

We have extended previous MC studies of particle size effects in supported metal catalysis to consider the influence of adsorbate diffusion, spillover and adsorption on the catalyst support. The model proposed by Zhdanov and Kasemo [11,12] for rapid heterogeneous catalytic reactions has been applied to a model hydrocarbon hydrogenation reaction occurring on a highly dispersed supported metal catalyst. It has been shown that if a reaction is rate limited by the adsorption of one of the components then the rate of that reaction can be expressed in terms of a modified ensemble model that takes into account the relative sizes of the hydrocarbon molecules and the metal particles. The influence of hydrogen spillover on the rate of the hydrogenation reaction was then shown to be negligible. We have also studied the extent to which a mean-field model for reaction with reactant supply from the support can be applied to disordered surfaces with a distribution of particle sizes. We have shown that, provided the density of particles on the catalyst support is low, the mean-field solution of the diffusion equation proposed by Routledge et al. [44] can be extended to describe the kinetics of CO oxidation occurring on a surface composed of a distribution of irregularly shaped particles.

Acknowledgements

A.S. McLeod thanks Peterhouse, Cambridge for the award of the Rolls-Royce Frank Whittle Research Fellowship and V.P. Zhdanov for helpful comments during the preparation of this manuscript.

References

[1] J.A. Dumesic, D.F. Rudd, L.M. Aparicio, J.E. Rekoske, A.A. Tervino, The Microkinetics of Heterogeneous Catalysis, American Chemical Society, Washington, 1992.
[2] M. Che, C.O. Bennett, Adv. Catal. 36 (1989) 55.
[3] C.O. Bennett, M. Che, J. Catal. 120 (1989) 2.
[4] G.A. Somorjai, Introduction to Surface Chemistry and Catalysis, Wiley, New York, 1994.
[5] V.P. Zhdanov, B. Kasemo, Surf. Sci. 405 (1998) 27.
[6] C.V. Ovesen, B.S. Clausen, J. Schiotz, P. Stoltze, H. Topsoe, J.K. Norskov, J.Catal 168 (1997) 133.
[7] V.P. Zhdanov, Elementary Physicochemical Processes on Solid Surfaces, Plenum, New York, 1991, p. 297.
[8] B. Delmon, G.F. Froment, Catal. Rev. Sci. Eng. 38 (1996) 69.
[9] D.-J. Kuan, H.T. Davies, R. Aris, Chem. Eng. Sci. 38 (1983) 719.
[10] R.I. Cukier, J. Chem. Phys 79 (1983) 2430.
[11] V.P. Zhdanov, B. Kasemo, Phys. Rev. B 55 (1997) 4105.
[12] V.P. Zhdanov, B. Kasemo, J. Catal. 170 (1997) 377.

[13] C. Becker, C.R. Henry, Surf. Sci. 352-354 (1996) 457.
[14] D. Linde, A. Mezhlumian, Phys. Rev. D 49 (1994) 1783.
[15] A.S. McLeod, K.Y. Cheah, L.F. Gladden, Stud. Surf. Sci. Catal. 118 (1998) 1.
[16] K. Kang, S.Redner, Phys. Rev. A 32 (1985) 435.
[17] M. Silverberg, A. Ben-Shaul, F. Robentrost, J. Chem. Phys. 83 (1985) 6501.
[18] M. Silverberg, A. Ben-Shaul, F. Robentrost, Surf. Sci. 214 (1989) 17.
[19] G. Ertl, Appl. Surf. Sci. 121 (1997) 20.
[20] A. Ahn, R. Kopelman, P. Argyrakis, J. Chem. Phys. 110 (1999) 2116.
[21] P.W. Jacobs, F.H. Ribeiro, G.A. Somorjai, S.J. Wind, Catal. Lett. 37 (1996) 131.
[22] P.L.J. Gunter, J.W. Niemantsverdriet, F.H. Ribeiro, G.A. Somorjai, Catal. Rev. Sci. Eng. 39 (1997) 77.
[23] C.R. Henry, Surf. Sci. Rep. 31 (1998) 231.
[24] W. Zhou, J.M. Thomas, D.S. Shephard, B.F.G. Johnson, D. Ozkaya, T. Maschmeyer, R.G. Bell, Q. Ge, Science 280 (1998) 705.
[25] A.S. McLeod, L.F. Gladden, J. Catal. 173 (1998) 43.
[26] R.M. Ziff, E. Gulari, Y. Barshad, Phys. Rev. Lett. 56 (1986) 2553.
[27] A.S. McLeod, L.F. Gladden, Catal Lett. 43 (1997) 189.
[28] A.S. McLeod, L.F. Gladden, J. Chem. Phys. 110 (1999) 4000.
[29] V.P. Zhdanov, B. Kasemo, Phys. Rev. Lett. 81 (1998) 2482.
[30] R.M. Nieminen, A.P.J. Jansen, Appl. Catal. 160 (1997) 99.
[31] K. Grass, H.G. Lintz, J. Catal. 172 (1997) 446.
[32] D. Duca, L. Botar, T. Vidoczy, J. Catal 162 (1996) 260.
[33] R.D. Cortright, S.A. Goddard, J.E. Rekoske, J.A. Dumesic, J. Catal. 127 (1992) 342.
[34] J.E. Rekoske, R.D. Cortright, S.A. Goddard, S.B. Sharma, J.A. Dumesic, J. Phys. Chem. 96 (1992) 1880.
[35] P.S. Cremer, G.A. Somorjai, J. Chem. Soc. Faraday Trans. 91 (1995) 3671.
[36] H.C. Kang, W.H. Weinberg, Chem. Rev. 95 (1995) 667.
[37] A.P.J. Jansen, J.J. Lukkien. This issue.
[38] S. Fortune, Algorithmica 2 (1987) 153.
[39] M.J. Yacaman, A. Gomez, Appl. Surf. Sci. 19 (1984) 348.
[40] G.A. Martin, Catal. Rev. Sci. Eng. 30 (1988) 519.
[41] F. Rumpf, H. Poppa, M. Boudart, Langmuir 4 (1988) 722.
[42] V. Matolín, E. Gillet, Surf. Sci. 166 (1986) L115.
[43] C.R. Henry, Surf. Sci. 223 (1989) 519.
[44] K.J. Routledge, M.J. Stowell, Thin Solid Films 6 (1970) 407.
[45] V. Matolin, I. Stará, Surf. Sci. 398 (1998) 117.